

Na₂V₃O₇: A Frustrated Nanotubular System with Spin-1/2 Diamond Ring Geometry

T. Saha-Dasgupta,¹ Roser Valentí,² F. Capraro,² and C. Gros²

¹*S. N. Bose National Centre for Basic Sciences, JD Block, Sector 3, Salt Lake City, Kolkata 700098, India*

²*Institut für Theoretische Physik, Universität Frankfurt, D-60438 Frankfurt, Germany*

(Received 23 September 2004; published 1 September 2005)

Following the recent discussion on the puzzling nature of the interactions in the nanotubular system Na₂V₃O₇, we present a detailed *ab initio* microscopic analysis of its electronic and magnetic properties. By means of a nontrivial downfolding study we propose an effective model in terms of tubes of nine-site rings with the geometry of a spin-diamond necklace with frustrated inter-ring interactions. We show that this model provides a quantitative account of the observed magnetic behavior.

DOI: 10.1103/PhysRevLett.95.107201

PACS numbers: 75.75.+a, 31.15.Ar, 75.25.+z

Introduction.—Low-dimensional quantum spin systems with chain, ladder, or planar geometries have attracted much attention in the last years [1] due to their unconventional magnetic properties. Recently substantial effort has been devoted to the search for new materials with exotic topologies and novel properties. For instance, the group of Millet *et al.* [2] has succeeded in synthesizing the first transition-metal-oxide-based nanotubular system Na₂V₃O₇. The discovery of Na₂V₃O₇ has introduced a new class of novel geometric structures in the field of magnetic nanostructures.

The V⁴⁺O₅ pyramids in Na₂V₃O₇ share edges and corners to form a nanotubular structure—a geometry first discovered for carbon—with Na atoms located inside and around each individual tube (see Fig. 1). The complex geometry of the compound is expected to provide nontrivial paths for the exchange interaction and hence to exhibit a nontrivial magnetic behavior. Initially this compound was predicted to be an example of a $S = 1/2$ nine-leg (or three-leg ladder) system with periodic boundary conditions along the rung direction [2]. Using the extended Hückel method, Whangbo and Koo [3] conjectured, on the other hand, that the tubes could be described by six mutually intersecting helical spin chains which should show a gap in the spin-excitation spectra.

Unlike antiferromagnetic (AF) spin ladders with even number of legs, the behavior of odd-leg ladders is strongly influenced by topology. An odd-leg ladder with open boundary conditions in the rung direction behaves effectively as a $S = 1/2$ AF Heisenberg chain and therefore shows no gap in the spin-excitation spectra. This situation changes dramatically when the boundary condition along the rung direction is periodic, as is the case for the spin tubes in Na₂V₃O₇. The introduction of periodic boundary conditions brings in an additional degree of freedom in the problem, namely, the chirality [4–7] and the ground state is then spontaneously dimerized with a gapped spectrum in all sectors. However, the magnetic properties of Na₂V₃O₇ as reported in the literature neither fit the properties of odd-leg spin tubes nor to that of helical spin chains as proposed by Whangbo and Koo [3] since no appreciable spin gap

could be detected in the susceptibility measurements [8]. A way out of this puzzling situation has been suggested by Lüscher *et al.* [9] by considering frustrated inter-ring couplings within the framework of a three-leg spin tube. While this surely provides an interesting model, its relevance for Na₂V₃O₇ remains yet to be examined.

Even though this compound has generated interest and controversy, no first-principles microscopic study has been reported so far. Our work in that respect is the first microscopic study carried out for Na₂V₃O₇. We have analyzed the *ab initio* density functional theory (DFT) results in terms of the newly developed Nth order muffin-tin orbital (NMO) based downfolding technique [10] to provide a microscopically derived spin model for Na₂V₃O₇. Our results show that the appropriate description of the system is that of tubes of nine-site rings with partially frustrated, next-nearest-neighbor intraring interactions and frustrated inter-ring interactions of weaker strength. Validity of this model is provided by the good agreement of our calculated susceptibility data with the measured data.

Ab initio Study.—Na₂V₃O₇ crystallizes [2] in the trigonal space group, $P31c$, with lattice constants, $a = 10.89$ Å and $c = 9.54$ Å. The unit cell contains six formula units. There are three inequivalent V sites (V1, V2, V3), seven

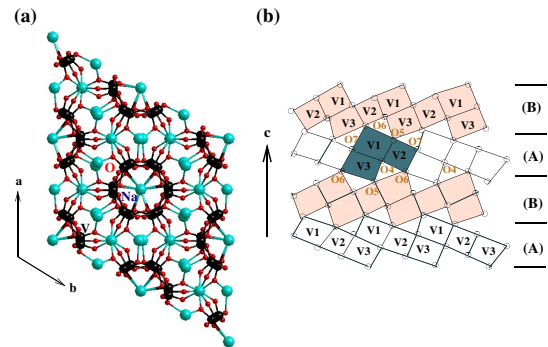


FIG. 1 (color online). Crystal structure of Na₂V₃O₇. (a) Projection on to (001) plane. V, Na, and O atoms are denoted by black, blue, and red balls, respectively. (b) Unfolded view of the edge and corner-sharing VO₅ pyramids within a tube.

inequivalent O sites (O1–O7), and four inequivalent Na sites (Na1–Na4). Each V is surrounded by five oxygen atoms with one characteristic short V-O bond giving rise to distorted square pyramids. The arrangement of VO₅ pyramids in a single tube is better viewed in the unfolded idealized representation of the nanotube as shown in Fig. 1(b). The edge-sharing VO₅ pyramids form nine-member rings out of the basic unit V1-V2-V3, in alternating sequence of (V2-V1-V3)-(V2-V1-V3)-(V2-V1-V3) and (V3-V1-V2)-(V3-V1-V2)-(V3-V1-V2) within slices (A) and (B). Rings in slices (A) and (B) are connected by the corner-sharing oxygens to form a nanotube of internal diameter of 5 Å, oriented along the crystallographic *c* direction [see Fig. 1(a)].

The DFT band structure in the generalized gradient approximation (GGA) [11], calculated using the linearized-muffin-tin-orbital (LMTO) method based on the Stuttgart TB-LMTO-47 code [12] and the linear augmented plane wave (LAPW) [13] method, consists of primarily O *p* and V *d*-derived bands in the region of interest [14]. The O *p*-dominated bands are separated by an energy gap of about 3 eV from the V *d*-dominated bands. The V *d*-dominated bands span an energy range of about 4 eV, starting from about -0.7 eV to 3.5 eV, with the zero of energy set at the GGA Fermi energy. The pyramidal coordination of oxygen atoms surrounding the V atom sets the V *xy d* orbital to be the lowest energy state within the V *d* manifold (in the local reference frame, with the *z* axis pointing along the shortest V-O bond and the *x* axis pointing along the next shorter V-O bond). The V *xy* bands therefore appear as *essentially* nonbonding set of bands extending from about -0.7eV to 0.4 eV. The crystal-field split V *yz*, *xz*, $3z^2 - 1$, and $x^2 - y^2$ complexes appear in the energy spectrum above the V *xy* complex in order of increasing energy. Na-derived states lie farther high up in energy with practically no mixing to bands close to the Fermi energy [15].

Starting from such a density-functional input, it is a nontrivial task to build up a low-energy model Hamiltonian relevant for the system. For the sake of uniqueness, however, it is essential for such model Hamiltonians to be derived in a first-principles manner containing the essential chemistry of the material. In recent years the Nth-order-muffin-tin-orbital-method-based [10] downfolding tech-

nique has been successful in achieving this goal [16]. The method relies on designing energy-selective Wannier-like effective orbitals by integrating out degrees of freedom that are not relevant—a method called *downfolding*. The few-orbital Hamiltonian is then constructed in the basis of these Wannier-like effective orbitals. In particular, in the present case, we integrate out all the degrees of freedom other than V *xy* orbitals. The effective V *xy* muffin tin orbitals (MTO's) generated in the process contains in its tail the integrated out O *p* and remaining V *d* orbitals, the weight being proportional to their mixing to V *xy*-derived bands. Fourier transform in the *downfolded* V *xy* basis gives the tight-binding Hamiltonian, $H_{\text{TB}} = \sum_{\langle i,j \rangle} t_{ij} (c_j^\dagger c_i + c_i^\dagger c_j)$ in terms of dominant V-V effective hopping integrals, t_{ij} , where *i* and *j* denote a pair of V⁴⁺ ions.

The nearest-neighbor (NN) V-V interactions within the V1-V2-V3 basic unit [marked by dark green in Fig. 1(b)] proceed via the edge-sharing oxygens while the intraring next nearest-neighbor (NNN) interactions proceed via corner-sharing oxygens [17]. Our first-principles-derived hopping integrals show that the edge-sharing NN V-V interactions within the V1-V2-V3 basic unit, t_1 , t_2 , and t_3 (see Fig. 2 and Table I), are of magnitude ranging from -0.14 eV to -0.18 eV. The NNN corner-sharing intraring interactions t'_1 and t'_2 are nearly equally strong. The interring V-V couplings $t_{i\perp}$, $t'_{i\perp}$ $i = 1, 2$ are an order of magnitude weaker than the intraring couplings. Nevertheless, we notice that the NNN inter-ring interactions ($t'_{1\perp}$ and $t'_{2\perp}$) are equally strong as the NN inter-ring interactions ($t_{1\perp}$ and $t_{2\perp}$). This induces inter-ring frustration which, as we will see later, could be of fundamental importance for the description of the magnetic behavior of the system at low temperatures.

This result is very different from the extended Hückel molecular-orbital-based result of Whangbo and Koo [3] which predicts that coupling via corner-sharing pyramids is much larger than that via edge sharing for Na₂V₃O₇. While this conclusion is in general true for vanadate systems like NaV₂O₅, LiV₂O₅, and CsV₂O₅ [18] it fails in the case of Na₂V₃O₇. Our result shows that the peculiar geometry of the VO₅ coordination, with marked deviation of the V-O-V bond angles from 180° and highly noncoplanar nature of V-O-V bonds, gives rise to coupling via edge sharing nearly equally strong as that via corner sharing as long as one is confined to a single ring. The magnitude of intraring, edge-sharing couplings are comparable to the largest edge-sharing hopping parameters in other vanadate

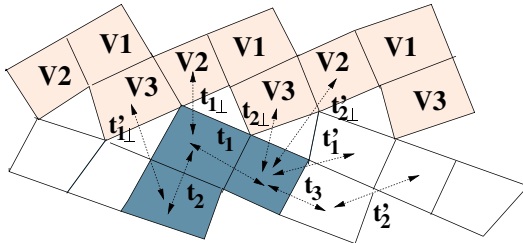


FIG. 2 (color online). Hopping parameters for Na₂V₃O₇ for V atoms belonging to slices (A) and (B) in Fig. 1(b). For identification of V atoms belonging to slice (A), refer to Fig. 1(b).

TABLE I. Inter- and intraring hopping integrals in eV. The next important hoppings are about 0.001 eV.

Intraring			Inter-ring					
t_1	t_2	t_3	t'_1	t'_2	$t_{1\perp}$	$t_{2\perp}$	$t'_{1\perp}$	$t'_{2\perp}$
-0.18	-0.15	-0.14	-0.13	-0.14	-0.03	-0.02	-0.02	-0.03

systems like CsV_2O_5 (-0.12 eV) [19] or LiV_2O_5 (-0.18 eV) [20] while the magnitude of intraring, corner-sharing couplings is much smaller than the largest corner-shared V-O-V in LiV_2O_5 or NaV_2O_5 which are about -0.3 eV [20,21]. The corner-sharing coupling between two adjacent rings is substantially diminished due to further misalignment of V xy orbitals belonging to two different rings which mixes the π character of the bond with that of δ character. In Fig. 3 we show the various *downfolded* V xy MTO's and their overlap giving us an idea of the influence of the distorted geometry on the relative orientations of the effective V xy orbitals, interaction paths, and the magnitude of overlaps.

Our microscopically derived hopping integrals show that $\text{Na}_2\text{V}_3\text{O}_7$ can be described as formed by tubes consisting of frustrated weakly coupled nine-site rings with *partial* intraring frustration. The *partial* frustration is due to the absence of the second neighbor V1-V3 interaction in the ring which is neither corner sharing nor edge sharing; rather it is decoupled by the intervening $\text{V}2(\text{O}_5)$ pyramid.

Susceptibility.—The exchange integral, J , can be expressed in general as a sum of antiferromagnetic and ferromagnetic contributions [22] $J = J^{\text{AF}} + J^{\text{FM}}$. In the strongly correlated limit, typically valid for transition metal oxides, the antiferromagnetic contributions are related to the hopping integrals, t_i , by using a perturbative approach as $J^{\text{AF}} = 4t_i^2/(U - \mathcal{V})$, where t_i corresponds to hopping via various V-O-V superexchange paths and U and \mathcal{V} are the on-site and intersite Coulomb interactions, respectively. In the absence of a generally accepted satisfactory way of direct computation of exchange integrals, such an approximate method is a good starting point for estimates of the exchange couplings as well as the relative strengths among the various exchange integrals [23].

In view of our *ab initio* results, the underlying spin-1/2 Hamiltonian for $\text{Na}_2\text{V}_3\text{O}_7$ can be written as

$$H = J_1 \sum_{i=1}^9 (\vec{S}_i \cdot \vec{S}_{i+1} + \alpha_i \vec{S}_i \cdot \vec{S}_{i+2}), \quad (1)$$

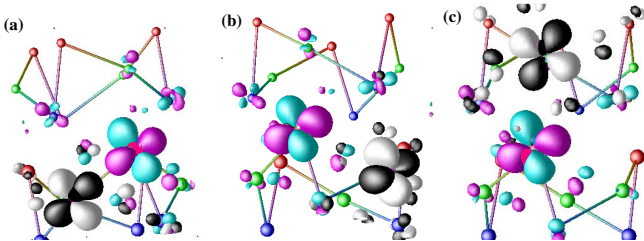


FIG. 3 (color online). Various intraring and inter-ring overlaps of the *downfolded* V xy MTO's at two V1 and V2 sites. Plotted are the orbital shapes (constant-amplitude surfaces) with the lobes of opposite signs labeled by black (magenta) and white (cyan) at site V1(V2). (a) Edge-sharing intraring, nearest-neighbor V1-V2 overlap (t_1). (b) Corner-sharing intraring, second neighbor V1-V2 overlap (t_1'). (c) Inter-ring V1-V2 overlap ($t_{1\perp}$).

where we neglect the small differences in between the three NN and two NNN intraring interactions and to a first approximation also neglect the small inter-ring couplings. $\alpha_i = J_2^i/J_1$ and we impose periodic boundary conditions $\vec{S}_{L+i} = \vec{S}_i$ ($L = 9$). In this model, the NNN coupling is inhomogeneously distributed in the sense that $\alpha_i = 0$ for $i = 1, 4, 7$ and $\alpha_i \neq 0 (= \alpha')$ for $i = 2, 3, 5, 6, 8, 9$ (see left illustration in Fig. 4). For a further check of the goodness of this model we considered in addition the fully frustrated model with $J_2^i = J_2$ for all i ($\alpha_i = \alpha$) (see right illustration in Fig. 4).

In Fig. 4 we present a comparison of the experimentally observed inverse magnetic susceptibility [8] with that obtained from exact diagonalization of the above-mentioned two kinds of frustrated models, varying the parameters J_1 as well as α or α' .

We observe that only the partially frustrated model ($\alpha' \neq 0$), which is the model predicted from the *ab initio* calculations with J_1 and J_2 antiferromagnetically signed, is able to reproduce the experimental data over the whole range of temperature. The fully frustrated model consistently shows, on the other hand, an upturn of the inverse susceptibility at lower temperatures not observed experimentally. We note here that estimates of J_1 and J_2 in terms of the downfolded t_i values [24] are within the same order of magnitude as those obtained here from the susceptibility comparison.

The partially frustrated model is invariant under translations $i \rightarrow i + 3$ ($i = 1, \dots, 9$) and corresponds therefore in the low-energy sector to a three-site ring with a fourfold degenerate ground state; i.e., it is a chirality-degenerate spin doublet [6]. The susceptibility of the partially frustrated model therefore diverges at low temperatures as $1/T$ (illustrated in Fig. 5). Below ~ 10 K the experimental susceptibility increases slower than the calculated one suggesting the absence of a spin gap. This is the range of energy where the inter-ring couplings, which have been neglected so far in our discussion, will start to be important (our *ab initio* $t_{\perp} = 0.03$ eV corresponds to a $J_{\perp} \sim 10$ K).

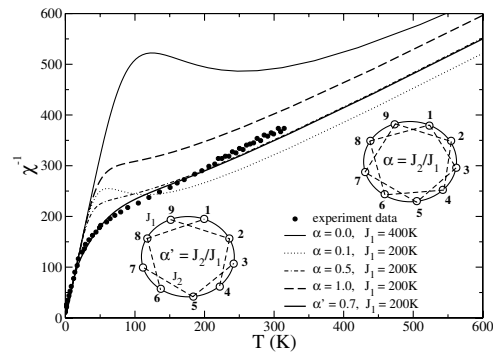


FIG. 4. Temperature dependence of the inverse magnetic susceptibility in units of mol/emu obtained from exact diagonalization for the two frustrated models of the inset [see Eq. (1)] compared with the experimental data [8] (filled dots).

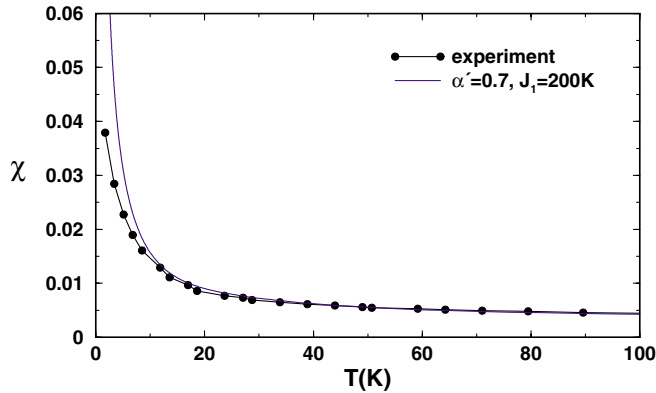


FIG. 5 (color online). Temperature dependence of the susceptibility (emu/mol) at low temperatures.

We consider in the following the contribution of the inter-ring couplings. Our *ab initio* results show that—though small—there are various contributions, $t_{1\perp}$, $t_{2\perp}$, $t'_{1\perp}$, and $t'_{2\perp}$, to the inter-ring coupling (see Table I and Fig. 2) which will be important at low temperatures and can compete against each other. These hoppings can be taken as a reference for the important exchange integrals to be considered, i.e., $J_{i\perp}$ and $J'_{i\perp}$. Assuming antiferromagnetic inter-ring couplings, consideration of only NN J_{\perp} will generally induce a spin gap [6] which will scale with the inter-ring exchange coupling. On the other hand, the existence of two competing exchange integrals J_{\perp} and J'_{\perp} , which induce inter-ring frustration, changes this scenario completely. As argued previously, the partially frustrated nine-site ring model corresponds in the low-energy sector to a three-site ring. We can therefore consider at low temperatures a model of three-site rings with frustrated inter-ring couplings which maps the main features extracted from our *ab initio* calculations. The recent density matrix renormalization group study by Lüscher *et al.* [9] on a tube of 3-site rings with frustrated inter-ring couplings showed that the spin gap diminishes if inter-ring frustration is present. For perfect frustration, i.e., $J_{\perp} = J'_{\perp}$, the spin gap goes exactly to zero since then we are left with an effective one-dimensional $S = 1/2$ Heisenberg model. Our *ab initio* hoppings t_{\perp} and t'_{\perp} are of the same strength which strongly points to the condition of almost complete frustration of the exchange integrals and therefore to a spin-gapless behavior as has been observed experimentally [8].

Finally, it is worth mentioning here that the partially frustrated nine-site ring model, for $\alpha' = 1$ and a large number of sites, is geometrically equivalent to the spin-1/2 diamond chain [25]. Our result $\alpha' = 0.7$ indicates that $\text{Na}_2\text{V}_3\text{O}_7$ is close to the spin-diamond geometry.

We acknowledge useful discussions with V.N. Muthukumar and J. Richter and the support of the Deutsche Forschungs Gemeinschaft. We thank the MPI-India partner group program for collaboration.

- [1] See, for a review, P. Lemmens, G. Güntherodt, and C. Gros, Phys. Rep. **375**, 1 (2003).
- [2] P. Millet, J. Y. Henry, F. Mila, and J. Galy, J. Solid State Chem. **147**, 676 (1999).
- [3] M.-H. Whangbo and H.-J. Koo, Solid State Commun. **115**, 675 (2000).
- [4] V. Subrahmanyam, Phys. Rev. B **50**, R16109 (1994).
- [5] H.J. Schulz in *Correlated Fermions and Transport of Mesoscopic System*, edited by T. Martin, G. Montambaux, and J. Tran Than Van (Frontieres, Gif sur Yvette, France, 1996).
- [6] K. Kawano and M. Takahashi, J. Phys. Soc. Jpn. **66**, 4001 (1997).
- [7] H.-T. Wang, Phys. Rev. B **64**, 174410 (2001).
- [8] J.L. Gavilano *et al.*, Phys. Rev. Lett. **90**, 167202 (2003).
- [9] A. Lüscher *et al.*, Phys. Rev. B **70**, 060405(R) (2004).
- [10] O.K. Andersen and T. Saha-Dasgupta, Phys. Rev. B **62**, R16219 (2000), and references therein.
- [11] J.P. Perdew, K. Burke, and M. Ernzerhof, Phys. Rev. Lett. **77**, 3865 (1996).
- [12] O.K. Andersen, Phys. Rev. B **12**, 3060 (1975).
- [13] P. Blaha, K. Schwarz, G. K. H. Madsen, D. Kvasnicka, and J. Luitz, computer code WIEN2K, 2001.
- [14] We checked convergence of the band-structure results obtained with the TB-LMTO scheme—where the down-folding procedure is implemented—versus the results from the full potential LAPW scheme.
- [15] We note that though the GGA calculations predict a metallic behavior for this system, since we have half-filled V-xy bands (corresponding to a V^{4+} in $3d^1$ configuration), it is to be expected that explicit inclusion of correlation effects through, e.g., an LDA + U calculation, will open a gap at the Fermi level and define the system as a Mott insulator.
- [16] See references in O. K. Andersen, T. Saha-Dasgupta, and S. Ezhov, Bulletin of Materials Science **26**, 19 (2003).
- [17] The first neighbor shell of intraring V-V pairs are of distances: 2.91 Å, 2.98 Å, and 3.06 Å. The next set of intraring interactions are of distances 3.71 and 3.55 Å.
- [18] Y. Ueda, Chem. Mater. **10**, 2653 (1998).
- [19] R. Valentí and T. Saha-Dasgupta, Phys. Rev. B **65**, 144445 (2002).
- [20] R. Valentí *et al.*, Phys. Rev. Lett. **86**, 5381 (2001).
- [21] V.V. Mazurenko *et al.*, Phys. Rev. B **66**, 081104(R) (2002).
- [22] H. Rosner *et al.*, Phys. Rev. Lett. **88**, 186405 (2002).
- [23] To be precise, one should add to J^{AF} the J^{FM} contribution as well, which may be estimated by evaluating the Coulomb exchange integrals between two Wannier functions centered at two neighboring sites. However, since we intend to extract from the *ab initio* calculation only the information of the important interaction paths which should define the relevant exchange paths, we have not included the FM contributions in our initial guess.
- [24] For a $U = 4$ eV typical for vanadates and neglecting \mathcal{V} , we obtain effective $J_1 = 285$ K and $J_2 = 211$ K. The ferromagnetic contribution -not included here- will renormalize this estimate. We note that the experimental J_1 is 200 K.
- [25] N. Fukushima, A. Honecker, S. Wessel, and W. Brenig, Phys. Rev. B **69**, 174430 (2004); S. K. Pati, S. Ramasesha, and D. Sen, Phys. Rev. B **55**, 8894 (1997).